



# Analysis of normal fault populations in the Kumano Forearc Basin, Nankai Trough, Japan: 1. Multiple orientations and generations of faults from 3-D coherency mapping

G. F. Moore and B. B. Boston

*Department of Geology and Geophysics, University of Hawai'i, 1680 East-West Rd., Honolulu, Hawaii 96822, USA (gmoore@hawaii.edu)*

A. F. Sacks and D. M. Saffer

*Department of Geosciences, Pennsylvania State University, 310 Deike Building, University Park, Pennsylvania, USA*

[1] Analyses of normal faults in the Kumano forearc basin of the Nankai Trough reveal multiple normal fault populations in a region generally thought to be under compression. Most faults have offsets of less than 20 m and dips of 60–70° and show no growth structures, indicating that the faults were active for short periods of time. The oldest generation of faults is older than ~0.9 Ma and strikes ~50–60°. The next oldest faults strike ~160–170°, are older than 0.44 Ma, and are related to local uplift along the western edge of the region. The youngest faults cut the seafloor; shallow faults near the SE margin of the basin curve from ~100° in the middle of the survey area to ~145° at the SE corner of the area. The pattern of the two youngest fault populations is consistent with the regional stress pattern (maximum horizontal stress subparallel to the trench). Orientations of older fault populations are caused by uplift of the underlying accretionary prism, implying that the forearc basin region is not as stable as previously thought. Reconstruction of displacements on the youngest faults shows that the overall horizontal extension is less than 2%, concentrated near the seaward edge of the basin. The active normal faults distributed throughout the basin support the idea that the horizontal stress parallel to the plate convergence direction does not reach the critical stress to activate or form thrust faults and produce horizontal shortening within the shallow portion of the inner wedge.

**Components:** 7,415 words, 13 figures, 1 table.

**Keywords:** Nankai Trough; forearc basin; normal fault.

**Index Terms:** 3060 Marine Geology and Geophysics: Subduction zone processes; 8104 Tectonophysics: Continental margins: convergent; 3025 Marine Geology and Geophysics: Marine seismics.

**Received** 24 September 2012; **Revised** 29 January 2013; **Accepted** 30 January 2013; **Published** 11 June 2013.

Moore, G. F., B. B. Boston, A. F. Sacks, and D. M. Saffer (2013), Analysis of normal fault populations in the Kumano Forearc Basin, Nankai Trough, Japan: 1. Multiple orientations and generations of faults from 3-D coherency mapping, *Geochem. Geophys. Geosyst.*, 114, 1989–2002, doi:10.1002/ggge.20119.

## 1. Introduction

[2] Forearc basins (FAB), prominent features of many convergent margins [Dickinson, 1995], are important not only because their sedimentary sections record the history of arc evolution but also because they record the history of deformation of the seaward edge of the overriding plate. Deformation of the upper plate is thought to affect the size and distribution of subduction zone earthquakes. For example, *Song and Simmons*, [2003] and *Wells et al.* [2003] suggest that seismic asperities on the subduction megathrust are correlated with forearc basins on the overriding plate, which implies that the configuration of the upper plate is linked to the seismic behavior of the underlying subduction thrust. *Rosenau and Oncken* [2009] also observe that FABs overlie areas of large megathrust earthquake slip. Those studies suggest that FABs are stable regions that overlie areas of large slip during megathrust earthquakes. *Wang and Hu* [2006] postulate that the actively deforming, most seaward part of an accretionary prism (the outer wedge) overlies the updip velocity-strengthening part of the subduction fault, and the less deformed inner wedge overlies the velocity-weakening part (the seismogenic zone). The inner wedge generally does not deform during earthquake cycles, acting as an apparent backstop and providing a stable environment for the formation of forearc basins. *Fuller et al.* [2006] suggest a link between processes controlling upper plate structure and seismic coupling on the subduction thrust. They point to a general lack of deformation in the forearc basin and suggest that the stability of the region increases the likelihood of thermal pressurization of the subduction thrust.

[3] Although the forearc regions of accretionary convergent margins are generally compressive environments [Dickinson, 2005], extensional normal faults characterize some FABs (e.g., Sumatra [Schlüter et al., 2002], Java [Kopp et al., 2009], and Nankai [Park et al., 2002; Gulick et al., 2010]). FAB extension may reflect long-term subsidence of the forearc due to sediment loading [Dickinson, 1995], a stable inner wedge that overlies the seismogenic plate interface and within which stresses vary over the seismic cycle [Wang and Hu, 2006], extension near the top of a critically tapered Coulomb wedge [Willett, 1999], permanent interseismic subsidence above the source zone [Wells et al., 2003], or uplift along the seaward margin of the basin [Park et al., 2002].

[4] In this paper, we identify multiple generations of normal faults in the Kumano forearc basin south of Honshu, Japan, quantify their orientations, and

demonstrate that they account for less than 2% of total extension across the basin. The second part of our study [Sacks et al., 2013] quantifies the regional stress state reflected by these fault populations.

## 2. Geologic and Tectonic Setting

[5] The Nankai Trough marks the plate boundary between the subducting Philippine Sea plate (PSP) and the Eurasian plate (Figure 1). The PSP is currently subducting to the NW at a rate of  $\sim 4.1\text{--}6.5\text{ cm yr}^{-1}$  [Seno et al., 1993; Miyazaki and Heki, 2001], with the convergence direction slightly oblique to the trench. Sediment accretion has been ongoing since at least the Cretaceous [Taira, 2001]. Currently all of the trench sediments and at least half of the underlying sedimentary section of the Shikoku Basin (northern PSP) are being accreted, forming a wide accretionary prism [e.g., Aoki et al., 1982; Moore et al., 1990]. Underthrusting of a large volume of the lower Shikoku Basin strata beneath the seaward edge of Kumano region [Bangs et al., 2009] is related to out-of-sequence thrusting along a regional megasplay fault that has uplifted a broad ridge, behind which the FAB has formed [Park et al., 2002].

[6] The Kumano Basin is a classic “ridged” FAB [e.g., Dickinson, 1995] bounded on its landward margin by an older accretionary prism (Shimanto Belt; Taira et al. [1988]) and on its seaward margin by the crest of the active accretionary prism and the Kumano Basin Edge Fault Zone (KBEFZ), a zone of complex normal and strike-slip faulting [Martin et al., 2010]. The basement of Kumano Basin comprises deformed upper Miocene and older accretionary prism rocks unconformably overlain by lower Pliocene trench slope deposits [Kinoshita et al., 2009]. Uplift along a regional megasplay fault began around 1.95 Ma, creating accommodation space for initiation of the forearc basin [Underwood and Moore, 2012]. The forearc basin strata are all younger than mid-Pleistocene (<2 Ma) in age [Kinoshita et al., 2009; Saffer et al., 2010]. More than 3 km of basin-filling sediment has been tilted landward, presumably due to continued slip on the megasplay fault [Gulick et al., 2010]. The basin strata are cut by numerous normal faults, many of which offset the seafloor (Figures 2 and 3) [Park et al., 2002; Moore et al., 2009; Gulick et al., 2010].

[7] The subducting Philippine Sea plate is characterized by regional and local variations in basement relief, sediment thickness, and sediment type [Ike et al., 2008a, 2008b]. Subduction of basement highs is known to cause significant deformation in

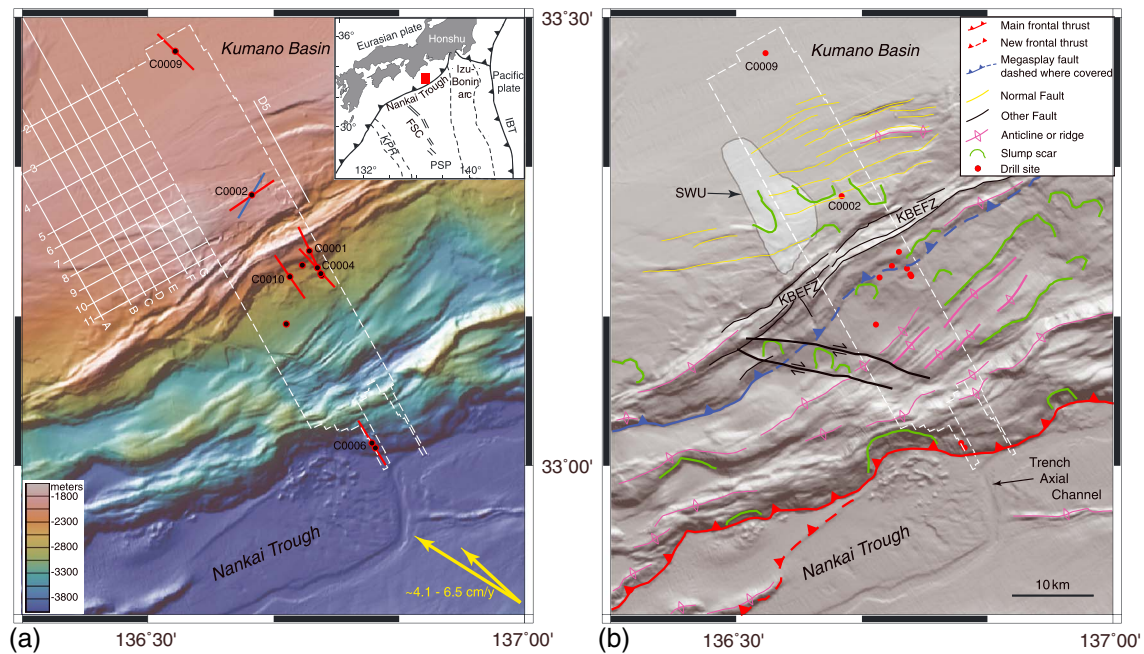


**Figure 1.** Shaded relief map of the Kumano Basin region of the Nankai Trough showing outline of 3-D seismic volume (white dashed box) and IODP drill sites (black dots). Red lines through labeled drill sites indicate maximum horizontal stress directions [Chang *et al.*, 2010; Lin *et al.*, 2010]. Blue line through Site C0002 indicates maximum horizontal stress direction below 936 m below seafloor. (a) Seabeam bathymetry also showing locations of JAMSTEC 2-D seismic lines (white lines). Yellow arrows show convergence vector between the Philippine Sea plate and Japan [Seno *et al.*, 1993; Heki, 2007]. Inset in upper right is a regional tectonic map showing the setting of the Nankai Trough study area. KPR = Kyushu-Palau Ridge; FSC = fossil spreading center; PSP = Philippine Sea Plate; IBT = Izu-Bonin Trench. Red box shows location of main map. (b) Tectonic interpretation (modified from Moore *et al.* [2009]). KBEFZ = Kumano Basin Edge Fault Zone [Martin *et al.*, 2010]; SWU = southwestern uplift.

the upper plate [e.g., von Huene, 2008], and subducted seamounts have been imaged under the Nankai forearc region [Park *et al.*, 1999; Kodaira *et al.*, 2000]. In addition, the large volume of

sediment that has been thrust under the megasplay fault in the Kumano region Bangs *et al.* [2009] may contribute to landward tilting of the forearc basin strata [Gulick *et al.*, 2010].

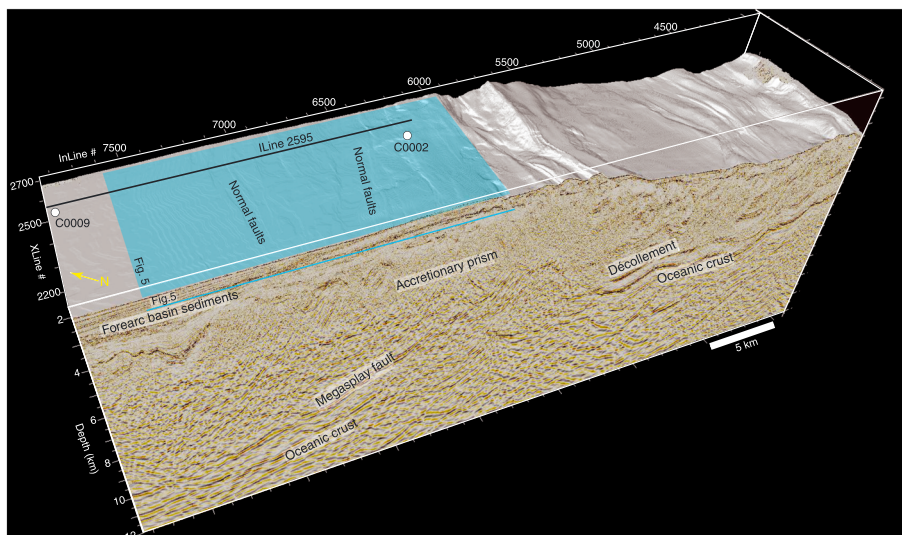


**Figure 2.** 3-D data cube showing regional extent of large normal faults on seafloor surface, locations of IODP drill sites in Kumano Basin and location of seismic Inline 2595. Blue shaded area is region covered by Figure 5, and blue line is the depth of the slice in Figure 5. Seismic data on cube face shows major tectonic features. Yellow arrow indicates north direction.

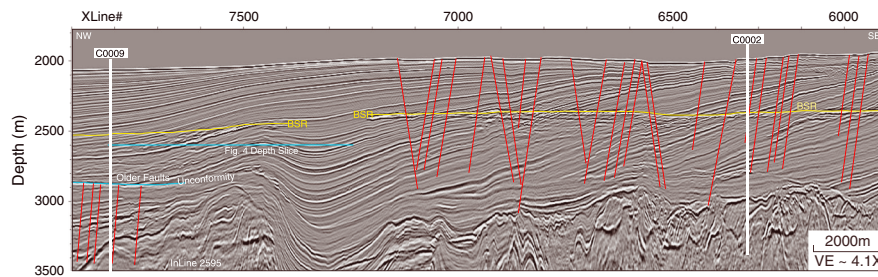


**Figure 3.** Seismic inline 2595 showing oldest (lower left) and youngest (right half of figure) forearc basin normal faults and location of IODP drill Sites C0002 and C0009. Blue line is depth of the slice in Figure 4. Location shown in Figure 2. BSR = bottom simulating reflection; VE = vertical exaggeration.

[8] Studies of borehole wall failures (borehole breakouts and drilling-induced tensile fractures) and anelastic strain recovery (ASR) in Integrated Ocean Drilling Program (IODP) drill holes across Kumano Basin show that the present-day stress state within the basin fill is predominantly in favor of normal faulting, with a maximum horizontal stress orientation that rotates from approximately perpendicular to the convergence vector between the Philippine Sea plate and Japan in the outermost basin, to nearly parallel to subduction by ~20 km landward (Figure 1) [Byrne *et al.*, 2009; Chang *et al.*, 2010; Lin *et al.*, 2010].

### 3. Data and Methods

[9] A 3-D seismic reflection data set was collected by Petroleum GeoServices (PGS) across the Kumano Basin and Nankai accretionary prism SE of Kii Peninsula in 2006 (Figure 1) [Moore *et al.*, 2007, 2009]. The 12 km wide, 56 km long survey

area covered the region from the trench axis landward into the Kumano Basin. Basic processing through prestack time migration was performed by Compagnie Générale de Géophysique (CGG), and full 3-D prestack depth migration (3-D PSDM) was completed by the Japan Agency for Marine Earth Science and Technology (JAMSTEC). We also used several 2-D seismic reflection lines collected by JAMSTEC in 2003 [Taira *et al.*, 2005] and 2004 to constrain the limits of normal faulting and tectonic uplift outside the 3-D survey box.

#### 3.1. Automatic Fault Extraction (AFE)

[10] This process uses cross correlation techniques on a 3-D volume to extract coherency. The coherence attribute is a measure of the similarity at each point in a seismic volume to its neighboring points. By calculating localized waveform similarity in both inline and crossline directions, estimates of 3-D seismic coherence are obtained [Bahorich and

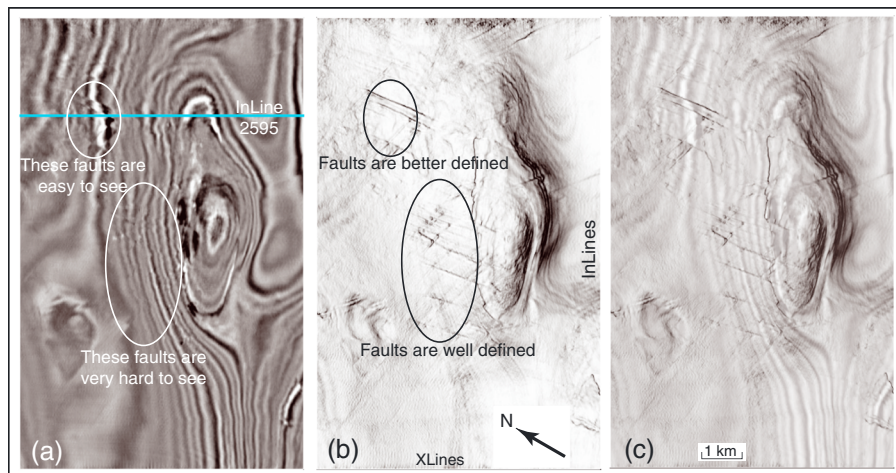


**Figure 4.** Map examples of seismic amplitudes versus coherency. Depth slices at 2600 m. Location of depth slice shown in Figure 3. (a) reflection amplitude; (b) coherency with high-coherence values in white, low-coherence values in black; (c) coherency superimposed on amplitude. Note how much easier the faults are to detect in the coherency displays.

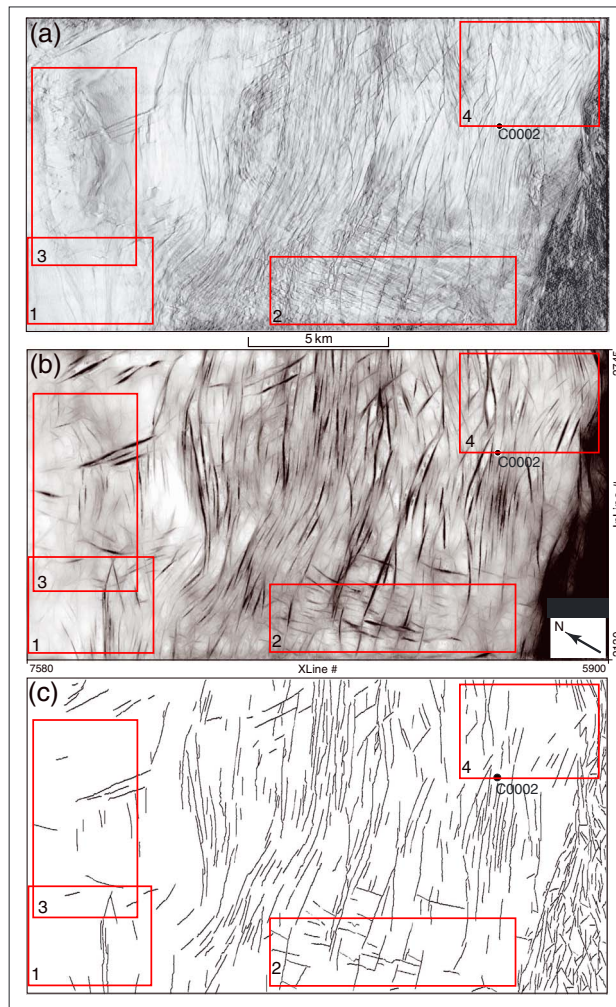


**Figure 5.** Depth slices at 2450 m with locations of normal fault population regions (shown in numbered boxes) used for analyses shown in Figure 6. (a) Coherency data; (b) line-enhanced processing; (c) fault-enhanced processing.

Farmer, 1995]. Coherence displays accentuate discontinuities in the input 3-D amplitude volume [Bahorich and Farmer, 1995; Marfurt *et al.*, 1998]. The processing produces a cube of coherence values between zero (no similarity between adjacent traces) and one (adjacent traces are identical) at each vertical sample point (every 5 m). Thus, trace-to-trace differences caused by a fault offset of a horizon result in a sharp discontinuity (near-zero coherence) that is expressed as a black line in our seismic displays (Figure 4).

[11] Small regions of seismic traces cut by a fault surface generally have a different seismic character than the corresponding regions of neighboring traces, resulting in a sharp discontinuity in local trace-to-trace coherence. Calculating coherence for each grid point along a depth slice results in lineaments of low coherence along faults, making them easily recognizable (Figure 5a).

[12] The first step of automatic fault extraction (AFE) attenuates any residual acquisition footprint (striping parallel to the acquisition direction) and enhances any lineaments by applying a destriping operator to estimate and remove any acquisition stripes on each depth slice (Figure 5b) [Dorn *et al.*, 2005; Dorn *et al.*, 2007]. This volume is then processed to enhance linear features, followed by fault enhancement and extraction of fault polylines on horizontal slices (Figure 5c). The fault polylines within a specified subvolume are then passed through automatic trend analysis, which outputs a rose diagram for the fault orientations (based on number of faults) in that subvolume over a 50 m depth interval (Figure 6).

[13] In a companion study, Sacks [2011] mapped 435 normal faults in the Kumano forearc basin using conventional workstation interpretation techniques. Her fault orientation and displacement

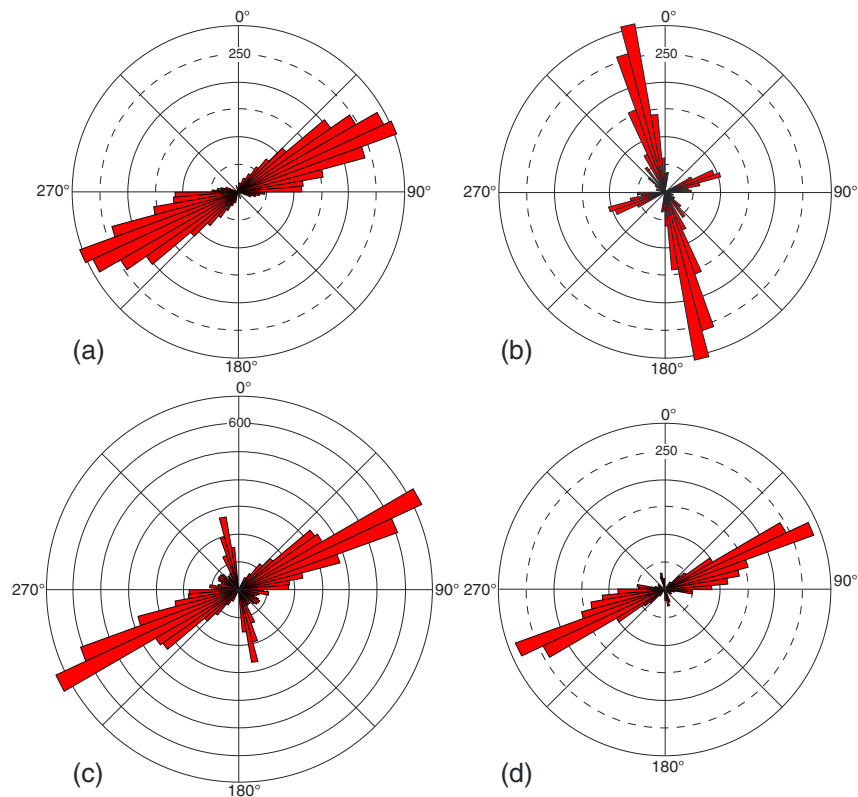


**Figure 6.** Rose diagrams showing fault azimuths in different regions and depths, reflecting different fault populations. Length of petals indicates number of faults within the region over a 50 m depth interval; circle interval for Figures 6a, 6b, 6d = 50; Figure 6c = 100. Region locations are shown in Figure 5. (a) Region 1 (NW corner; 3075–3125 m); (b) region 2 (SW edge; 2175–2225 m); (c) region 3 (N-central region; 2175–2225 m); (d) region 4 (SE portion of forearc basin; 2200–2250 m).

measurements [Sacks *et al.*, 2013] are nearly identical to the AFE values presented here, confirming the accuracy of the automated technique.

### 3.2. Fault Displacement Analysis

[14] To obtain quantitative estimates of fault displacement, we employed two different techniques. Displacement restoration using LithoTect<sup>®</sup> software was performed at the University of Hawaii. In this process, fault offsets of individual horizons are reversed using graphical restoration algorithms [e.g., Geiser *et al.*, 1988; Rowan and Kligfield, 1989; Rowan and Ratliff, 2012]: bed-length restoration preserves the line lengths of horizons; vertical simple shear and inclined simple shear maintain the lengths of vertical or inclined lines, respectively; fault-parallel slip keeps imaginary lines parallel to a given fault at a constant length; rigid-body rotation maintains the exact shape and size of fault blocks; and area restoration relaxes the other constraints while still preserving unit area.

[15] In the second fault displacement analysis, carried out as part of the companion study [Sacks *et al.*, 2013], the location and magnitude of heave of each fault along transects parallel to the convergence direction were recorded. Incremental heave along each transect was then calculated, and heaves for each mapped fault were summed to obtain the absolute magnitude of cumulative extension [Sacks *et al.* 2013]. The results of the two different analyses produced very similar results (see Table 1).

## 4. Normal Faults in the Kumano Forearc Basin

### 4.1. Fault Populations

[16] Several populations of normal faults have been recognized in Kumano Basin (Figures 2, 3, and 5). Most faults within the FAB have apparent throws (vertical separation) of less than 15 m, with throw appearing to decrease with depth. Although the faults that appear to decrease in throw with depth

**Table 1.** Summary of Extensional Strain Analysis on Seismic Inlines

Inline #	Method	Restored	Total	Total
		Length (m)	Extension (m)	Strain (%)
2235	CH	13863	128	0.9
2291	LT	12822	122	0.95
2455	CH	15475	277	1.8
2525	LT	15233	243	1.6
2645	CH	15613	236	1.5
2645	LT	15531	222	1.4

(CH=calculated heave; LT=Lithotect).

may simply have offsets that are below the resolution of the data in the deep part of the basin [Gulick *et al.*, 2010], normal faulting is the dominant mode of brittle strain in the shallow portion of the accretionary prism at IODP Site C0002 [Lewis *et al.*, 2013], indicating that the normal faults extend below the base of the FAB strata.

[17] Gulick *et al.* [2010] recognized four normal fault populations that offset the main forearc basin strata. Most of the faults dip steeply ( $53\text{--}58^\circ$ ), are generally planar, and are not associated with any growth strata. Sacks [2011] determined that fault dips average  $58^\circ$  ( $\sigma = 5^\circ$ ), with a range from  $45^\circ$  to  $82^\circ$ . Landward-dipping faults comprise 70% of the total population, and although the mean dip angle is identical, they generally exhibit a narrower range of dips than the seaward-dipping faults, particularly in the seaward portion of the basin. Many of the faults cut the seafloor, testifying to their youth [Gulick *et al.*, 2010]. We have recognized two additional fault populations, one older than the main basin-filling strata and one recent, but not active, population associated with continued deformation of the underlying accretionary prism.

[18] The oldest normal fault population (phase 1) is restricted to the NW part of the basin (region 1 in Figure 5) and does not cut a regional seismic surface dated at 0.9 Ma in IODP Hole C0009A [Saffer *et al.*, 2010] (Figures 7 and 8). The faults strike NE-SW ( $045\text{--}090^\circ$ ; Figure 6), generally dip  $65\text{--}75^\circ$ , and extend for 3–5 km. The zone of faulting is 7.5 km long, extending to the NW edge of the 3-D survey box. The width is about 12.5 km, from ~inline 2320 in the 3-D survey, extending westward to 2-D Line D (Figure 1b). The maximum throw is 18 m, but most of the faults have throws of ~10–12 m, which is near the limit of seismic resolution for this depth. These faults are all generally planar, with little or no curvature with depth and no indication of growth structures.

[19] A younger population of planar faults (phase 2) along the west side of the survey (region 2 in Figure 5) strike NW-SE and are continuous for 1.5–3.25 km. This zone of faulting is at least 6 km wide, extending from ~2.75 km west of the west edge of the survey inboard 3.25 km (inline 2130–2320); it is 7 km long, extending from the KBEFZ to the middle of basin (crossline 6140–6915).

[20] The phase 2 faults (Figure 9) do not cut the blue horizon (equivalent to “Top Kumano 4” of Gulick *et al.* [2010]) in Figure 10, which we traced to the location of IODP drill Site C0009. Nannofossils from cuttings at this depth yield an age of 0.436 Ma [Saffer *et al.*, 2010]. These faults are spatially correlated with uplift along the SW edge of the survey area (Figure 1b). This fault population was considered by Gulick *et al.* [2010] to be part of their group 4, but we believe that they are a separate group because they are planar and are

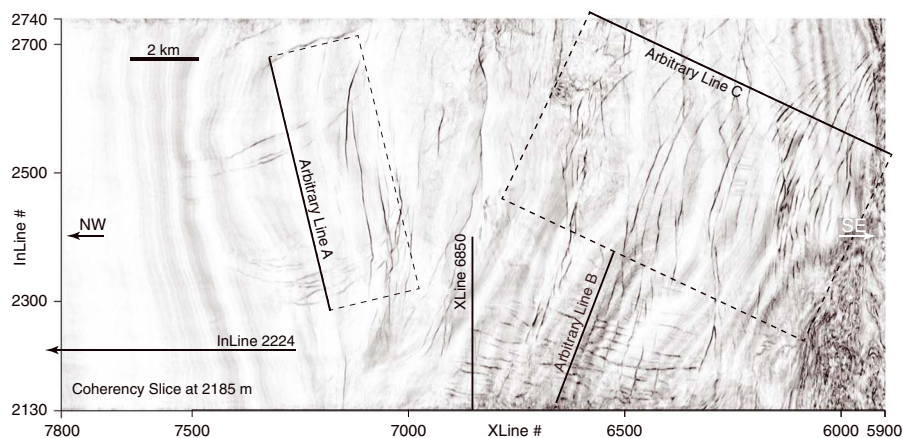


**Figure 7.** Coherency slice at 2185 m showing locations of seismic lines in later figures. Dashed lines show dimensions of depth slices associated with arbitrary lines in Figures 11 and 12.

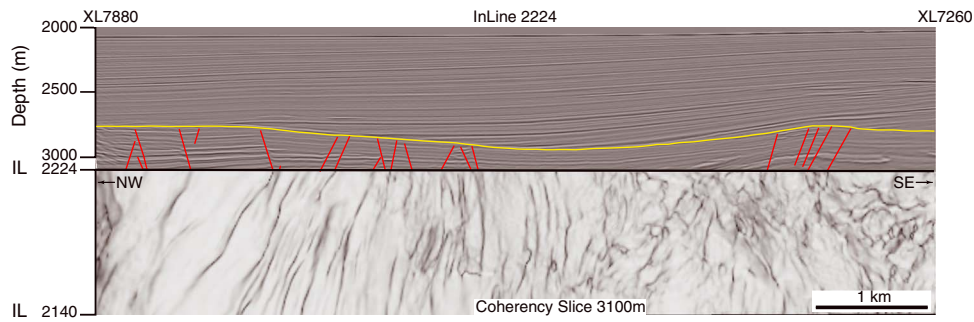


**Figure 8.** Coherency depth slice of region 1 (Figure 5) at 3100 m with seismic inline 2224 showing the oldest normal fault population that strikes NE-SW and does not cut the 0.9 Ma unconformity (yellow line).

restricted to the west side of the survey, whereas the group 4 faults are equivalent to our phase 3 faults (described next).

[21] The third fault group (phase 3) contains arcuate faults (Figure 5, region 3; Figures 7–11) with an 80° range of strikes from 085° to 165°. In this population, the seawardmost faults strike nearly E-W, whereas the landward-most faults strike nearly N-S. This subset of faults occurs primarily in the northern, landward portion of the survey, where the forearc basin sediment package thickens. These faults exhibit the smallest maximum offsets of any subgroup, averaging about 8 m. Their traces in the coherency data are not smooth but are rather jagged compared to the faults that cut them (Figure 11). Although these faults come very close to the seafloor, none of them have any expression in the seafloor topography (Figure 1), so we consider them to be inactive. These jagged NW-SE-striking faults are cross-cut by younger, less jagged NE-SW-striking faults (Figure 11).

[22] The youngest faults (phase 4) in the basin strike NE-SW and cut the seafloor, indicating that this fault population has been recently active. The faults are

planar in cross-section at a large scale (Figure 3) and have two subpopulations. One is generally linear in map view, and the second is arcuate in map view (Figures 5–7). The linear faults are generally smooth in the coherency displays in the NW part of the basin, where they form large, regionally continuous graben (Figure 1). Near the SE side of the 3-D box, they become more jagged (Figure 12). The maximum throw is 30 m but is <10 m on most of the faults.

[23] The arcuate phase 4 faults curve, with strikes varying from ~060° to ~085° in the southeastern corner of the 3-D box. The faults are generally planar and approximately parallel in cross-section but, when displayed at increased scale, are nonplanar and nonparallel at a small scale. In most cases, the arcuate faults cut the linear faults (Figure 12), but there are also examples of the linear faults cutting the arcuate faults, so we consider the two populations to be contemporaneous. None of the NE-SW-striking faults extend into the NW-most part of basin, which is the current depocenter, so we cannot determine whether the faults cut the youngest basin sediments, which would imply that they are still active.

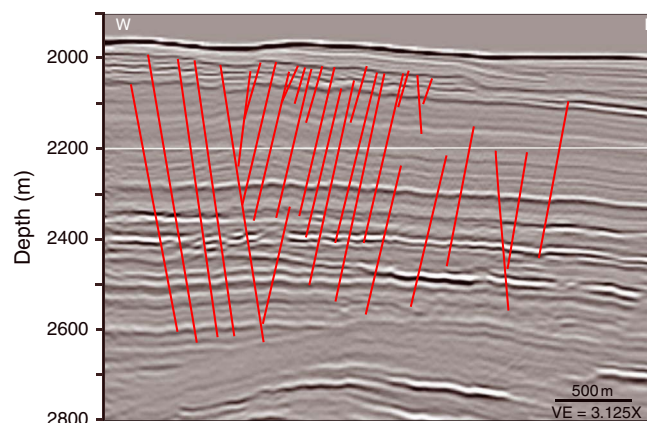


**Figure 9.** Arbitrary line B showing nature of faulting NW-striking fault system along SW edge of survey (region 2; Figure 5).

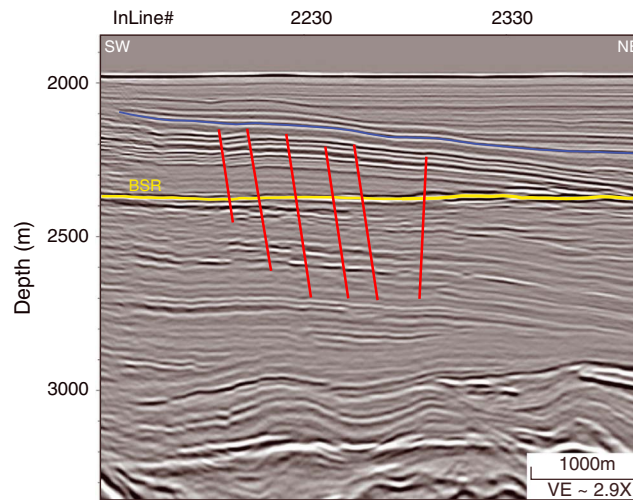


**Figure 10.** Crossline 6850 showing that region 2 faults shown in Figure 9 do not cut the blue horizon, which correlates with cuttings data at Site C0009 to give an age of 0.436 Ma. Yellow line highlights the bottom simulating reflection (BSR). Note that reflections below the BSR dip to the right (NE) due to uplift along the SW edge of the 3-D survey. The youngest reflections are horizontal and onlap above the blue horizon.

#### 4.2. Fault Relays and Hourglass Structures

[24] The youngest fault population is characterized by many intersecting faults that have a conjugate geometry in the profile view. Some of these faults form relay ramps [e.g., *Morley et al.*, 1990; *Peacock and Sanderson*, 1994] and “X” or hourglass structures (Figure 13) [e.g., *Bretan et al.*, 1996; *Nicol et al.*, 1995]. Animation S1 (in the supporting information)<sup>1</sup> shows both of these structures in an animation that steps sequentially through a series of seismic inlines. In cross-section, the faults are nearly planar.

[25] On the left side of the animation, the surface defines a relay ramp, which is unbreached. The animation shows that, while the relay-bounding faults are subparallel and nearly constant in dip with depth, their traces are variable at short distances along strike: the separation between the faults is variable, and faults coalesce. On the right side of the animation, the seismic lines show the interaction between landward- and seaward-dipping faults that form an hourglass structure (Figure 13). The upper portion of the structure is a graben, while the lower part is a horst. Along strike, the interactions between the faults change rapidly, and the structure disappears. Note that the landward-dipping fault is offset by the seaward-dipping fault, indicating that it is older. The landward-dipping fault also does not cut the seafloor, while the seaward-dipping fault does

cut the seafloor. However, landward of the hourglass structure, there are two additional landward-dipping faults, both of which cut the seafloor. We thus infer that the seaward-dipping and landward-dipping subpopulations grew nearly synchronously.

#### 4.3. Fault Restoration and Strain Analysis

[26] We carried out LithoTect restorations of the youngest normal faults along three inlines (2291, 2525, and 2645) and manual analysis of fault heaves along three inlines (2235, 2455, and 2645). The average strike of this fault system is  $\sim 065\text{--}075^\circ$ , which is within  $5\text{--}15^\circ$  of perpendicular to our inline direction (Figures 5 and 6), so we performed our analyses on the inlines (Table 1). Small errors ( $< \sim 5\%$ ) can be introduced by being slightly off perpendicular, but we do not believe that these errors affect the overall conclusions.

[27] The overall extension along mapped faults due to the youngest phase of fault activity averages 1.35%, with a range of 0.9–1.8% in the inline direction (approximately parallel to the regional subduction vector; Figure 1). We are able to detect many small-offset faults in the seismic data, but a magnitude of the offsets are too small to be quantifiable. Including these structures would increase the total extension slightly, so our strain estimates should be considered as minimum values. Although the inlines are essentially normal to the fault strikes, if slip on the normal faults is not pure dip-slip, the orientation of the true

<sup>1</sup>Additional supporting information may be found in the online version of this article.

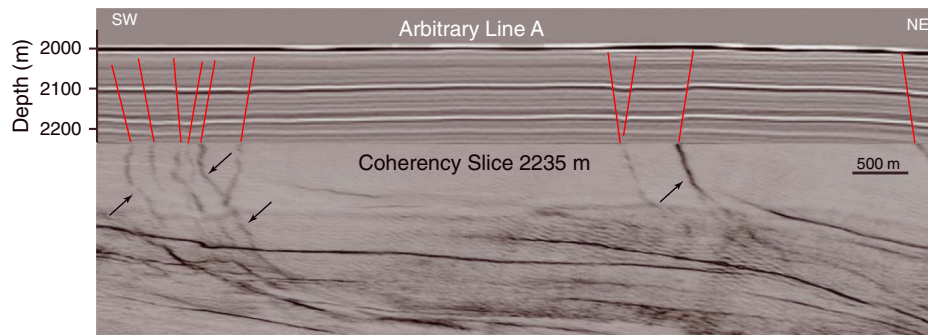


**Figure 11.** Seismic line and coherency slice showing the nature of NW-SE-striking faults in region 3 (Figure 5). Arrows point to “jagged” faults. Location of seismic line shown in Figure 7.

maximum extension could be oblique to the inline direction, and the magnitude of maximum extension would also be slightly larger than we report.

## 5. Discussion

### 5.1. Fault Populations

[28] We identified four phases of normal faulting in the Kumano FAB. The two oldest fault populations are the result of deformation in the underlying accretionary complex that continued after the FAB sediments were deposited. Phase 1 faults (NE-SW-striking faults that are restricted to the NW end of the survey) are associated with an anticline-syncline at depth (Figure 8) and are older than 0.9 Ma. Phase 2 faults (NW-SE faults along the SW edge of the 3-D survey) are associated with a broad regional uplift (“SWU” in Figure 1) that extends NW parallel to the 3-D box. These faults are older than a 0.436 Ma surface. This surface is

tilted NE about  $1^\circ$  along the SWU and landward about  $2^\circ$  due to the regional tilting. Thus, both phase 1 and 2 faults occurred during the latest period of regional tilting [Gulick *et al.*, 2010] but were primarily associated with deformation of the underlying accretionary prism. These faults thus reflect the local stress field generated in response to nearby structures, rather than the regional stress regime at the time of their formation.

[29] The youngest faults cut all older structures, are regionally significant (they extend across the basin; Figure 1), and cut the seafloor. They thus reflect the recent stress state (the subject of the companion paper by Sacks *et al.* [2013]).

### 5.2. Hourglass Structures and Relay Zones

[30] Cross-cutting sets of fault planes (conjugates) that form “hourglass” structures are common features of normal fault systems [e.g., Nicol *et al.*, 1995; Bretan *et al.*, 1996]. An important question

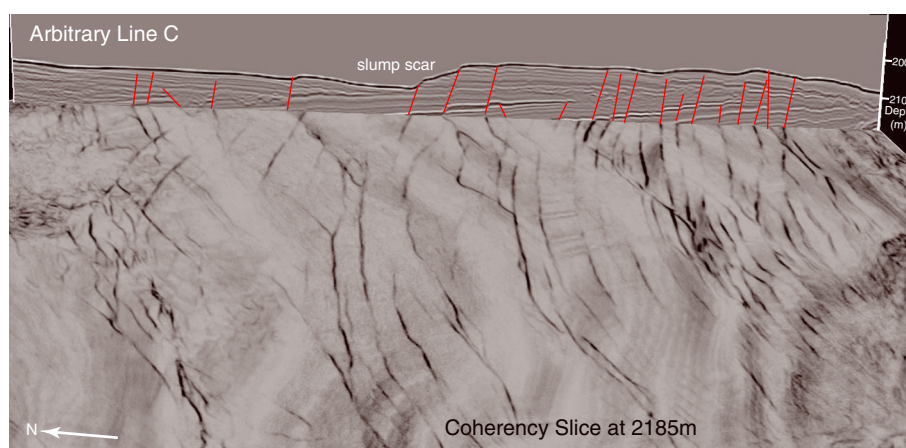


**Figure 12.** Seismic line and coherency slice showing nature of youngest faults in region 4 Figure 5. Location of seismic line shown in Figure 7.

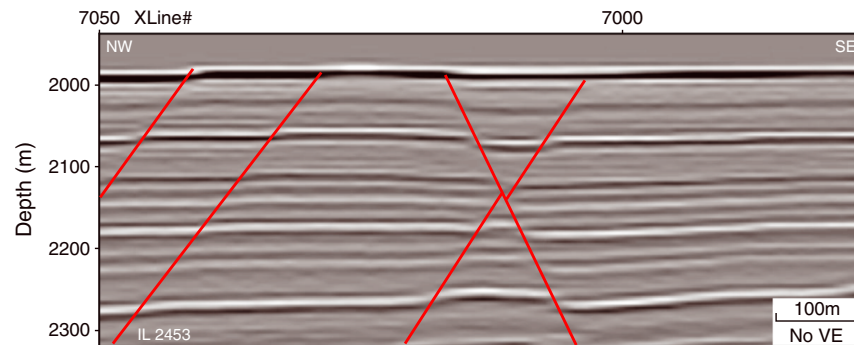


**Figure 13.** Seismic inline showing “X” or “hourglass” structure.

concerning hourglass structures is whether the conjugate faults form by incidental intersection of independent nucleated, oppositely dipping faults, or by nucleation and growth from an intersection point [Nicol *et al.*, 1995]. The origin of conjugate structures in the Timor Sea area was attributed to incidental intersections of opposite-dipping faults in which the dimensions, location, and displacement patterns of the future conjugate-fault pairs were unrelated [Nicol *et al.*, 1995; Bretan *et al.*, 1996]. Çiftçi and Langhi [2012], however, believe that the Timor Sea hourglass structures formed by two different phases of extension with different stress fields. The youngest phase of faults in Kumano Basin exhibits such structures and may be of interest because most of these faults cut the seafloor, indicating that they are either currently active or were active within the past few hundred years. We point out, however, that subseismic deformation at the intersections of the synchronous conjugate normal faults cannot be resolved in our seismic data [e.g., Nicol *et al.*, 1995; Watterson *et al.*, 1998].

[31] Displacements on normal faults are usually partitioned between interacting fault segments. The displacement transfer from one fault segment to another segment that dips in the same direction most often occurs through relay structures [e.g., Peacock and Sanderson, 1994; Childs *et al.*, 1995, 1996; Walsh *et al.* 1999]. Walsh *et al.* [2003] suggest that relay zones most often form with fault segments as components of a single kinematically coherent system. In this model, each fault segment initiates as a component of a spatially and mechanically related array. This implies that the formation of a relay zone is geologically instantaneous (i.e., formation is on a time scale that is less than the temporal resolution of the growth data) and that the faults bounding the relay zone always formed a kinematically coherent system. This is the case with the relays ramps in the Kumano Basin.

[32] Relay ramp growth in Kumano Basin has not progressed beyond the early stage of stable ramp configuration with minor ramp rotation. Growth has not yet reached the ramp breaching stage [e.g., Imber *et al.*, 2004], so that the rotation of bedding in the ramps is very small ( $<0.5^\circ$ ; the change in depth is 3–5 m over 1000–1200 m).

### 5.3. Fault Orientations and Regional Stresses

[33] The active and recent normal faults in Kumano Basin indicate that the modern stress regime reflects regional horizontal extension approximately parallel to the present convergence vector. This is consistent with stress magnitudes obtained from analyses of borehole breakout width [Chang *et al.*, 2010; Lin *et al.*, 2010], ASR measurements [Byrne *et al.*, 2009], and predictions of the stress regime from numerical modeling studies investigating the effects of splay faults [Conin *et al.*, 2012].

[34] The orientations of the two youngest normal fault populations are broadly consistent with the regional maximum horizontal principal stress ( $S_{Hmax}$ ) direction inferred from borehole wall failure orientations at IODP Sites C0002 [Chang *et al.*, 2010] and C0009 [Lin *et al.*, 2010] and from stress inversions for core-scale faults at Site C0002 [Lewis *et al.*, 2013]. The dominant fault orientation (strike) in the seaward part of the basin near Site C0002 is NE-SW, consistent with the observed NE-SW  $S_{Hmax}$  orientation. Landward in the basin, in the vicinity of Site C0009, the phase 2 fault population, which strikes primarily NW-SE, is consistent with the inferred NW-SE  $S_{Hmax}$  direction at this location [Lin *et al.*, 2010]. The orientation of  $S_{Hmax}$  in the deeper part of section at Site C0002 is also inferred to be NW-SE. Thus, stresses likely rotate with depth to transition from the normal faulting regime in the upper few kilometers

to a compressional (thrust faulting) regime in the wedge interior [e.g., *Chang et al.*, 2010].

[35] Our results showing the dominance of normal faulting and absence of thrust faulting in the FAB strata are noteworthy because they indicate that, although the underlying accretionary prism remains under compression perpendicular to the convergence direction, these compressive stresses are not transmitted up into the forearc basin. Moreover, when topographic highs on the subducting oceanic basement pass beneath the basin, they cause deformation (mostly uplift) of the overlying accretionary prism, but uplift causes normal faulting within the FAB. Furthermore, the short-lived nature of the normal faults indicated by the lack of growth structures implies that normal faulting in the shallow levels of the FAB is not a long-term regional phenomenon.

## 6. Conclusions

[36] Normal faults in Kumano Basin document several phases of faulting in the FAB, providing a record of both recent regional stress patterns and timing and localization of deformation in the FAB “basement” (the underlying accretionary prism). None of the faults show any growth characteristics, indicating that they were short-lived features. Phase 1 faults strike NE-SW and are associated with thrust faulting within the underlying accretionary prism in the NW region of the basin prior to 0.9 Ma [*Boston et al.*, 2011]. Phase 2 faults strike NW-SE and reflect broad regional uplift along the western edge of the 3-D box prior to 0.436 Ma. Both of these faulting phases point to continued thrusting within the underlying accretionary prism, possibly due to subduction of basement highs.

[37] The youngest two phases of faults are regionally extensive, and the fault orientations are consistent with stress information from borehole breakouts and ASR measurements indicating stretching perpendicular to the regional convergence vector.

[38] The abundant, recent, and active normal faults distributed throughout the basin support the idea that the within the shallow portion of the inner wedge, the horizontal stress parallel to the plate convergence direction does not reach the critical stress to activate or form thrust faults and produce horizontal shortening. It is unclear how this changes with depth and whether this transitions to a compressive, thrust faulting stress regime at greater depths, but the lack of compressional deformation in the basin could reflect decoupling of stress and strain between the younger, softer,

weaker basin fill and the underlying accretionary wedge due to contrasts in mechanical strength across the unconformity. Alternatively, the entire inner wedge may be either stable or in extension [*Wang and Hu*, 2006], except when disrupted by topographic highs on the subducting plate.

## Acknowledgments

[39] This project was supported by the National Science Foundation (grant #s OCE-0451790 and OCE-0451602). We thank R. Ratliff for help with LithoTect and S. Martel for discussions on normal faulting. Helpful reviews by T. Byrne, M. Conin, J. Lewis, C. Moore, A. Nicol, and M. Withjack greatly improved the manuscript. We are grateful to Landmark Graphics (Haliburton) and Paradigm Geophysical for academic software grants that made this work possible. SOEST Contribution # 8822.

## References

- Aoki, Y., T. Tamano, and S. Kato (1982), Detailed structure of the Nankai Trough from migrated seismic sections. in *Studies in Continental Margin Geology*, edited by J. S. Watkins and C. L. Drake, *Am. Assoc. Petrol. Geol. Mem.*, 34, 309–322.
- Bahorich, M., and S. Farmer (1995), The coherence cube, *Leading Edge*, 14, 1053–1058.
- Bangs, N. L. B., G. F. Moore, S. P. S. Gulick, E. M. Pangborn, H. J. Tobin, S. Kuramoto, and A. Taira (2009), Broad, weak regions of the Nankai megathrust and implications for shallow coseismic slip, *Earth Planet. Sci. Lett.*, 284, 44–49.
- Boston, B., J. Barnes, and Moore, G. F. (2011), Buried accretionary thrusts beneath the Kumano forearc basin, SW Japan, Abstract T51F-2413 presented at 2011 Fall Meeting, AGU, San Francisco, Calif., 5–9 Dec.
- Bretan, P. G., A. Nicol, J. J. Walsh, and J. Watterson (1996), Origin of some conjugate or “X” fault structures, *The Leading Edge*, 15, 812–816.
- Byrne, T. B., et al. (2009), Anelastic strain recovery reveals extension across SW Japan subduction zone, *Geophys. Res. Lett.*, 36, L23310, doi:10.1029/2009gl040749.
- Chang, C., L. C. McNeill, J. C. Moore, W. Lin, M. Conin, Y. Yamada (2010), In situ stress state in the Nankai accretionary wedge estimated from borehole wall failures, *Geochem. Geophys. Geosyst.*, 11, Q0AD04, doi:10.1029/2010GC003261.
- Childs, C., J. Watterson, and J. J. Walsh (1995), Fault overlap zones within developing normal fault systems, *J. Geol. Soc.*, 152, 535–549.
- Childs, C., J. Watterson, and J. J. Walsh (1996), A model for the structure and development of fault zones, *J. Geol. Soc.*, 153, 337–340.
- Çiftçi, N. B., and L. Langhi (2012), Evolution of the hourglass structures in the Laminaria High, Timor Sea: Implications for hydrocarbon traps, *J. Struct. Geol.*, 36, 55–70.
- Conin, M., P. Henry, V. Godard, and S. Bourlange (2012), Splay fault slip in a subduction margin, a new model of evolution, *Earth Planet. Sci. Lett.*, 341–344, 170–175.
- Dickinson, W. R. (1995), Forearc basins, in *Tectonics of Sedimentary Basins*, edited by C. J. Busby and R. V. Ingersoll, 221–261, Blackwell, Cambridge, MA.

- Dorn, G. A., H. E. James, D. Dopkin, and B. Payne (2005), Automatic fault extraction in 3D seismic interpretation, *67th EAGE Conference Expanded Abstracts, F035*, 4 pp.
- Dorn, G. A., H. E. James, L. Evins, J. Marbach, and F. A. Coady (2007), Applications of Automatic Fault Extraction (AFE) in a variety of geologic environments: Results, limitations and suggested improvements, *Am. Assoc. Petrol. Geol. Bull. (Ann. Meeting Abs.)*.
- Fuller, C. W., S. D. Willett, and M. T. Brandon (2006), Formation of forearc basins and their influence on subduction zone earthquakes, *Geology*, *34*, 65–68.
- Geiser, J., P. A. Geiser, R. Kligfield, R. A. Ratliff, and M. G. Rowan (1988), New applications of computer-based cross section construction: strain analysis, local balancing and subsurface fault prediction, *Mountain Geol.*, *25*, 47–59.
- Gulick, S. P. S. et al. (2010), Rapid forearc basin uplift and megasplay fault development from 3D seismic images of Nankai Margin off Kii Peninsula, Japan, *Earth Planet. Sci. Lett.*, *300*, 55–62.
- Heki, K. (2007), Scular, transient and seasonal crustal movements in Japan from a dense GPS array: Implications for plate dynamics in convergent boundaries, in *The Seismogenic Zone of Subduction Thrust Faults*, edited by T. Dixon and C. Moore, pp. 512–539, Columbia University Press, New York, NY.
- von Huene, R. (2008), When seamounts subduct, *Science*, *321*, 1165–1166.
- Ike, T., G. F. Moore, S. Kuramoto, J.-O. Park, Y. Kaneda, and A. Taira (2008a), Variations in sediment thickness and type along the northern Philippine Sea Plate at the Nankai Trough, *Island Arc*, *17*, 342–357.
- Ike, T., G. F. Moore, S. Kuramoto, J.-O. Park, Y. Kaneda, and A. Taira (2008b), Tectonics and sedimentation around Kashinosaki Knoll: A subducting basement high in the eastern Nankai Trough, *Island Arc*, *17*, 358–375.
- Imber, J., G. W. Tuckwell, C. Childs, J. J. Walsh, T. Manzocchi, A. E. Heath, C. G. Bonson, and J. Strand (2004), Three-dimensional distinct element modelling of relay growth and breaching along normal faults, *J. Struct. Geol.*, *26*, 1897–1911.
- Kinoshita, M., H. Tobin, J. Ashi, G. Kimura, S. Lallemand, E. J. Screaton, D. Curewitz, H. Masago, M. K. Thu, and the Expedition 314/315/316 Scientists edited by (2009), Proc. IODP. Integrated Ocean Drilling Program Management International, Inc., College Station, TX.
- Kodaira, S., Y. Kaneda, N. Takahashi, A. Nakanishi, and S. Miura (2000), Subducted seamount imaged in the rupture zone of the 1946 Nankaido earthquake, *Science*, *289*, 104–106.
- Kopp, H., D. Hindle, D. Klaeschen, O. Oncken, C. Reichert, and D. Scholl (2009), Anatomy of the western Java plate interface from depth-migrated seismic images, *Earth Planet. Sci. Lett.*, *288*, 399–407.
- Lewis, J., T. Byrne, and K. Kanagawa (2013), Evidence for mechanical decoupling of the upper plate at the Nankai subduction zone: Constraints from core-scale faults at NantroSEIZE sites C0001 and C0002, *Geochem. Geophys. Geosyst.*, doi:10.1029/2012GC004406, in press.
- Lin, W., et al. (2010), Present-day principal horizontal stress orientations in the Kumano forearc basin of the southwest Japan subduction zone determined from IODP NanTroSEIZE drilling Site C0009, *Geophys. Res. Lett.*, *37*, L13303, doi: 10.1029/2010gl043158.
- Marfurt, K. J., R. L. Kirlin, S. L. Farmer, and M. S. Bahorich (1998), 3-D seismic attributes using a semblance-based coherency algorithm, *Geophysics*, *63*, 1150–1165.
- Martin, K. M. et al. (2010), Possible strain partitioning structure between the Kumano fore-arc basin and the slope of the Nankai Trough accretionary prism, *Geochem. Geophys. Geosyst.*, *11*, Q0AD02. doi: 10.1029/2009gc002668.
- Miyazaki, S. I., and K. Heki (2001), Crustal velocity field of southwest Japan: Subduction and arc-arc collision, *J. Geophys. Res.*, *106*, 4305–4326.
- Moore, G. F., N. L. Bangs, A. Taira, S. Kuramoto, E. Pangborn, and H. J. Tobin (2007), Three-dimensional splay fault geometry and implications for tsunami generation, *Science*, *318*, 1128–1131.
- Moore, G. F., et al. (1990), Structure of the Nankai Trough accretionary zone from multichannel seismic-reflection data, *J. Geophys. Res.*, *95*, 8753–8765.
- Moore, G. F., et al. (2009), Structural and seismic stratigraphic framework of the NanTroSEIZE Stage 1 transect, in: Kinoshita, M., Tobin, H., Ashi, J., Kimura, G., Lallemand, S., Screaton, E. J., Curewitz, D., Masago, H., Moe, K. T., and the Expedition 314/315/316 Scientists (Ed.), Proc. IODP. Integrated Ocean Drilling Program Management International, Inc., College Station, TX.
- Morley, C. K., R. A. Nelson, T. L. Patton, and S. G. Munn (1990), Transfer zones in the East African rift system and their relevance to hydrocarbon exploration in rifts, *Am. Assoc. Petrol. Geol. Bull.*, *74*, 1234–1253.
- Nicol, A., J. J. Walsh, J. Watterson, and P. G. Bretan (1995), Three-dimensional geometry and growth of conjugate normal faults, *J. Struct. Geol.*, *17*, 847–862.
- Park, J. O., Y. Kaneda, T. Tsuru, S. Kodaira, and P. R. Cummins (2002), Splay fault branching along the Nankai subduction zone, *Science*, *297*, 1157–1160.
- Park, J. O., S. Kodaira, N. Takahashi, H. Kinoshita, T. Tsuru, Y. Kaneda, and Y. Kono (1999), A subducting seamount beneath the Nankai accretionary prism off Shikoku, southwestern Japan, *Geophys. Res. Lett.*, *26*, 931–934.
- Peacock, D. C. P., and D. J. Sanderson (1994), Geometry and development of relay ramps in normal fault systems, *Am. Assoc. Petrol. Geol. Bull.*, *78*, 147–165.
- Rosenau, M., and O. Oncken (2009), Fore-arc deformation controls frequency-size distribution of megathrust earthquakes in subduction zones, *J. Geophys. Res.*, *114*, B10311, doi:10.1029/2009JB006359.
- Rowan, M. G., and R. Kligfield (1989), Cross section restoration and balancing as aid to seismic interpretation in extensional terranes, *Am. Assoc. Petrol. Geol. Bulletin*, *73*, 955–966.
- Rowan, M. G., and R. A. Ratliff (2012), Cross-section restoration of salt-related deformation: Best practices and potential pitfalls, *J. Struct. Geol.*, *41*, p. 24–37, doi:10.1016/j.jsg.2011.12.012.
- Sacks, A. F. (2011), Principal axes of stress and strain in the Kumano Forearc Basin from inversion of a normal fault population mapped in a 3D seismic volume, Nankai Trough, SW Japan. M.S. Thesis, College of Earth and Mineral Sciences, Pennsylvania State University, State College, PA, 85 pp.
- Sacks, A. F., D. M. Saffer, and D. M. Fisher (2013), Analysis of normal fault populations in the Kumano Forearc Basin, Nankai Trough, Japan: 2. Principal axes of stress and strain from inversion of fault orientations, *Geochem. Geophys. Geosyst.*, *14*.
- Saffer, D., L. McNeill, T. Byrne, E. Araki, S. Toczko, N. Eguchi, K. Takahashi, and the Expedition 319 Scientists (2010), Proc. IODP, 319: Tokyo (Integrated Ocean Drilling Program Management International, Inc.), doi:10.2204/iodp.proc.319.101.2010.
- Schlüter, H. U., C. Gaedicke, H. A. Roeser, B. Schreckenberger, H. Meyer, C. Reichert, Y. Djajadihardja, and A. Prexl (2002), Tectonic features of the southern Sumatra-western Java forearc of Indonesia, *Tectonics*, *21*, 1047, doi:10.1029/2001TC901048.



- Seno, T., S. Stein, and A. E. Gripp (1993), A model for the motion of the Philippine Sea plate consistent with NUVEL-1 and geological data, *J. Geophys. Res.*, *98*, 17941–17948.
- Song, T.-R. M., and M. Simons (2003), Large trench-parallel gravity variations predict seismogenic behavior in subduction zones, *Science*, *301*, 630–633.
- Taira, A. (2001), Tectonic evolution of the Japanese Island Arc System, *Ann. Rev. Earth Planet. Sci.*, *29*, 109–134.
- Taira, A., J. Katto, M. Tashiro, M. Okamura, and K. Kodama (1988), The Shimanto Belt in Shikoku Japan: Evolution of a Cretaceous to Miocene accretionary prism, *Modern Geol.*, *12*, 5–46.
- Taira, A., D. Curewitz, et al., (2005), CDEX Technical Report, V.1:Nankai Trough seismogenic zone site survey: Kumano Basin seismic survey, Philippine Sea, Offshore Kii Peninsula, *Ann. Rev. Earth Planet. Sci.*, *25*(8), 64 pp.
- Underwood, M. B., and G. F. Moore (2012), Evolution of sedimentary environments in the subduction zone of southwest Japan: Recent results from the NanTroSEIZE Kumano transect, in *Tectonics of Sedimentary Basins: Recent Advances*, edited by C. J. Busby and A. P. Azor, pp. 310–326, Wiley-Blackwell, New York.
- Walsh, J. J., J. Watterson, W. R. Bailey, and C. Childs (1999), Fault relays, bends and branch-lines, *J. Struct. Geol.*, *21*, 1019–1026.
- Walsh, J. J., W. R. Bailey, C. Childs, A. Nicol, and C. G. Bonson (2003), Formation of segmented normal faults: a 3-D perspective, *Journal of Structural Geology*, *25*(8), 1251–1262.
- Wang, K., and Y. Hu (2006), Accretionary prisms in subduction earthquake cycles: The theory of dynamic Coulomb wedge, *J. Geophys. Res.*, *111*, B06410, doi:10.1029/2005JB004094.
- Watterson, J., A. Nicol, and J. J. Walsh (1998), Strains at the intersections of synchronous conjugate normal faults, *J. Struct. Geol.*, *20*, 363–370.
- Wells, R. E., R. J. Blakely, Y. Sugiyama, Y. D. W. Scholl, and P. A. Dinterman (2003), Basin-centered asperities in great subduction zone earthquakes: A link between slip, subsidence, and subduction erosion?, *J. Geophys. Res.*, *108*, B02507, doi:10.1029/2002JB002072.
- Willett, S. D. (1999), Rheological dependence of extension in wedge models of convergent orogens, *Tectonophysics*, *305*, 419–435, doi:10.1016/S0040-1951(99)00034-7.